Shear Buckling of Specially Orthotropic Plates with Centrally Located Cutouts

Eric C. Klang; Principle Investigator
Vicki Owen; Graduate Student

Mechanical and Aerospace Engineering
North Carolina State University
Raleigh, NC 27695-7910

1. Introduction

The purpose of this project is to analyze the shear loading of a composite rectangular plate with a centrally located circular cutout in order to predict the buckling load of the plate. The first step in this analysis is to calculate the in-plane stress distribution of the plate prior to buckling. This problem can be solved using finite element methods, but a quicker and more cost efficient method is desired. The method chosen to determine the pre-buckling stresses is that of boundary collocation using complex variables. The real valued force functions are written in terms of two complex valued functions, each of which is a function of a different complex variable. The solution of the generalized biharmonic function is a superposition of functions of these two complex variables.

For this analysis, the force functions are represented with Laurent series. The constants in these series are found using boundary collocation. Two force equations for complex variables are satisfied over the plate boundaries to obtain these constants. The stresses in the plate are then known for any particular locations on the plate given the applied shear on the edges of the plate.

2. Analysis

For a two dimensional stress analysis, the equilibrium equations are:

$$\frac{\partial \sigma_{xx}}{\partial x} + \frac{\partial \tau_{xy}}{\partial y} = 0$$

$$\frac{\partial \sigma_{yy}}{\partial y} + \frac{\partial \tau_{xy}}{\partial x} = 0$$

(1)

The solutions for the stresses in terms of a function F are:

$$\sigma_{xx} = \frac{\partial^2 F}{\partial y^2} \qquad \sigma_{yy} = \frac{\partial^2 F}{\partial x^2} \qquad \tau_{xy} = -\frac{\partial^2 F}{\partial x \partial y}$$

(2)

Writing the generalized biharmonic equation in terms of the stress function F gives:

$$\frac{1}{E_x} \frac{\partial^4 F}{\partial y^4} - \frac{2\eta_{xy,x}}{E_x} \frac{\partial^4 F}{\partial y^3 \partial x} - \left(\frac{2\nu_{xy}}{E_x} - \frac{1}{G_{xy}} \right) \frac{\partial^4 F}{\partial y^2 \partial x^2} - \frac{2\eta_{xy,y}}{E_y} \frac{\partial^4 F}{\partial y \partial x^3} + \frac{1}{E_y} \frac{\partial^4 F}{\partial x^4} = 0$$

(3)

Defining:

$$z_1 = x + \mu_1 y \qquad z_2 = x + \mu_2 y$$

$$\frac{\partial}{\partial z} = \frac{\partial}{\partial y} - \mu_k \frac{\partial}{\partial x} \qquad\qquad k = 1, 2$$

(4)

where μ_k are the roots of the characteristic equation:

$$\mu^4 - 2\eta_{xy,x} \mu^3 + \left(\frac{E_x}{G_{xy}} - 2\nu_{xy} \right) \mu^2 - 2\eta_{xy,y} \frac{E_x}{E_y} \mu + \frac{E_x}{E_y} = 0$$

(5)

The generalized biharmonic equation can be represented as:

$$\frac{\partial}{\partial z_1} \frac{\partial}{\partial z_2} \frac{\partial}{\partial z_1} \frac{\partial}{\partial z_2} F = 0$$

(6)

the solution for F being:

$$F = \phi_1(z_1) + \phi_2(z_2) + \overline{\phi_1(z_1)} + \overline{\phi_2(z_2)}$$

(7)

Substituting F back into the stress equations and letting $\Phi_k(z_k) = \partial\phi_k/\partial z_k$ gives:

$$\sigma_x = \frac{\partial^2 F}{\partial y^2} = 2*\text{Re}\ (\mu_1^2\ \Phi_1' + \mu_2^2\Phi_2')$$

$$\sigma_y = \frac{\partial^2 F}{\partial x^2} = 2*\text{Re}\ (\Phi_1' + \Phi_2')$$

$$\tau_{xy} = -\frac{\partial^2 F}{\partial x \partial y} = -2*\text{Re}\ (\mu_1\Phi_1' + \mu_2\Phi_2')$$

(8)

Two force equation can be written using the function $\_k$:

$$2*\text{Re}\ [\Phi_1(z_1) + \Phi_2(z_2)]\ \Big|_{\zeta_o}^{\xi} = \pm\left(-\int_0^S Y_n ds\right)$$

$$2*\text{Re}\ [\mu_1\Phi_1(z_1) + \mu_2\Phi_2(z_2)]\ \Big|_{\zeta_o}^{\xi} = \pm\int_0^S X_n ds$$

(9)

where the upper sign applies to external contours, the lower sign applies to internal contours, and s is the arclength of a segment on the boundary originating at ℓ_o and ending at ℓ. X_n and Y_n are the forces applied to the boundary in the x and y directions respectively. For this analysis, the force function Φ_k will be represented by a Laurent series of 2*N terms written as follows:

$$\Phi_k(z_k) = \sum_{-N}^{N} A_{kn}\ \xi_k^n$$

(10)

where A_{kn} is a complex number, $c_{kn} + id_{kn}$.

Substituting the series representation for Φ_k into the force equation and evaluation from i to i-1 gives:

$$2*\text{Re}\left[\sum_{-N}^{N}\{(c_{1n} + i\,d_{1n})(\xi_{1i}^n - \xi_{1(i-1)}^n) + (c_{2n} + i\,d_{2n})(\xi_{2i}^n - \xi_{2(i-1)}^n)\}\right] = \pm\ (-Y_n S)$$

$$2*\text{Re}\left[\sum_{-N}^{N}\{\mu_1(c_{1n} + i\,d_{1n})(\xi_{1i}^n - \xi_{1(i-1)}^n) + \mu_2(c_{2n} + i\,d_{2n})(\xi_{2i}^n - \xi_{2(i-1)}^n)\}\right] = \pm X_n S$$

(11&12)

Multiplying out the left hand side of equation (11) and finding the real part of the expressing gives:

$$\sum_{-N}^{N} \{c_{1n}(2*\mathrm{Re}\,(\xi_{1i}^{n} - \xi_{1(i-1)}^{n})) + d_{1n}(-2*\mathrm{Im}\,(\xi_{1i}^{n} - \xi_{1(i-1)}^{n})) +$$

$$c_{2n}(2*\mathrm{Re}\,(\xi_{2i}^{n} - \xi_{2(i-1)}^{n})) + d_{2n}(-2*\mathrm{Im}\,(\xi_{2i}^{n} - \xi_{2(i-1)}^{n}))\} = \pm (-Y_n S) \qquad (13)$$

Similarly for equation (12):

$$\sum_{-N}^{N} \{c_{1n}(2*\mathrm{Re}\,(\mu_1(\xi_{1i}^{n} - \xi_{1(i-1)}^{n}))) + d_{1n}(-2*\mathrm{Im}\,(\mu_1(\xi_{1i}^{n} - \xi_{1(i-1)}^{n}))) +$$

$$c_{2n}(2*\mathrm{Re}(\mu_2(\xi_{2i}^{n} - \xi_{2(i-1)}^{n}))) + d_{2n}(-2*\mathrm{Im}(\mu_2(\xi_{2i}^{n} - \xi_{2(i-1)}^{n})))\} = \pm X_n S \qquad (14)$$

For n=0, ζ_{1i} - $\zeta_{1(i-1)}$ = 1-1 = 0 and the same for ζ_2, therefore the coefficients A_{10} and A_{20} are arbitrary, thus the Laurent series for Φ_k becomes:

$$\Phi_k = \sum_{-N}^{-1} A_{kn}\xi_k^n + \sum_{1}^{N} A_{kn}\xi_k^n \qquad (15)$$

The term ξ_k is determined by mapping z_k in such a manner as to improve the conditioning of the system of equations generated by this method. For this analysis, the cutout will be mapped onto a unit circle using the mapping function:

$$\xi_k = \frac{z_k}{(a - i\mu_k b)}\left(1 + \frac{\sqrt{z_k^2 - a^2 - \mu_k^2 b^2}}{z_k}\right) \qquad (16)$$

where a and b are the semi-major and semi-minor axes of an ellipse.

Solving the force boundary conditions around the internal and external boundaries of the plate results in a system of equations which can be arranged in matrix form as follows:

$$[\,C_{kn}\,]\,\{A_k\} = \{F_n\}$$

where the A_k are the unknown constants, C_{kn} are the coefficients of the constants over each segment, and F_n are the resultant forces applied over the segment. To improve the solution of this system of equations, a least squares approach is taken. Using this method, twice as many equations will be used as there are unknowns. Therefore:

$[\,C_{kn}\,]$ is a 16*N x 8*N matrix
$\{A_k\}$ is a 8*N vector
$\{F_n\}$ is a 16*N vector

To solve this system, each side of the system is multiplied by $[\,C_{kn}\,]^T$ as follows:

$$[\,C_{kn}\,]^T\,[\,C_{kn}\,]\,\{\,A_{kn}\,\} = [\,C_{kn}\,]^T\,\{\,F_n\,\}$$

Now there are an equal number of equations and unknowns and the system can be solved directly for the unknown constants. Substituting these constants into ϕ_k and differentiating gives the solution for this function in terms of x and y. Therefore, we now have a solution for the stresses in the plate in terms of x and y.

3. Results

To solve for the pre-buckling stresses in a plate with a circular cutout under shear loading, a general program was written that allows for future expansion. This program can handle a rectangular or elliptical cutouts rotated at some given angle. It will also handle normal loading in the x and y directions as well as shear.

Shown in figures 1-3 are the pre-buckling normal and shear stress distributions for an isotropic plate with a circular cutout under shear loading. The plate has dimensions l=w=1.0" with a cutout of radius 0.15". Figure 4 shows the changes in the shear distribution for a hole of increased radius, and figure 5 exhibits the changes that occur when the material properties of the plate are non-isotropic. Figure 6 displays the shear stress distribution for the isotropic plate with and elliptical cutout, and figure 8 shows the same plate with the cutout rotated at a 45° angle to the x-axis. Figure 7 shows the shear stress distribution in the plate corresponding to a square cutout.

To examine how the complex variable boundary collocation method compares to infinite theory, four plots were made. Each plot is based on an isotropic plate with a circular cutout under shear loading. The radius of the hole was varied from 0.01" to 0.15" in the plots shown in figures 9-12. The plots track the changes in shear stress along the x-axis from the edge of the cutout to the edge of the plate. As the radius of the hole decreases, the boundary collocation method results converge to the infinite solution. The same results can be shown for the plate loaded in tension in the y-direction. As the radius of the cutout decreases, at the edge of the hole, the stress in the y-direction divided by the value of the loading, σ_{yy}/P_2, approaches 3 as predicted by infinite theory for an isotropic plate. This is shown in figure 13.

In finalizing the pre-buckling section of the program, a decision must be made on the desired number of terms in the Laurent series. For:

$$\Phi_k = \sum_{-N}^{-1} A_{kn}\xi_k^n + \sum_{1}^{N} A_{kn}\xi_k^n$$

a value must be chosen for N. Figure 14 indicates how the solution approaches the finite element solution for shear stress along the x-axis from the edge of the cutout to the edge of the plate as N increases. In this case, the cutout is a circle of radius 0.15". Although increasing N increases the accuracy of the solution, is also decreases the range of D/W for which a solution is possible. Worst case scenarios were run through the program, and the following values of N were decided upon:

$$1.04\% \leq D/W^* \leq 30\% \quad N=5$$

$$30\% \leq D/W^* \leq 60\% \quad N=8$$

where D is the hole diameter and W^* is the length of the longest side. It is desired that a length to width ratio (L/W) of 4 be possible. For this condition:

$$4.16\& \leq D/W \leq 30\%$$

is possible where W is the actual width of the plate.

4. Future Goals

To complete the pre-buckling problem, more finite element comparisons will be made to verify the solution. Contour plots of the finite element solution will be made to compare with the plots in figures 1-8.

One more option will also be added to the program. The program will be written so that displacements can be prescribed along the boundaries as opposed to the forces being specified if desired.
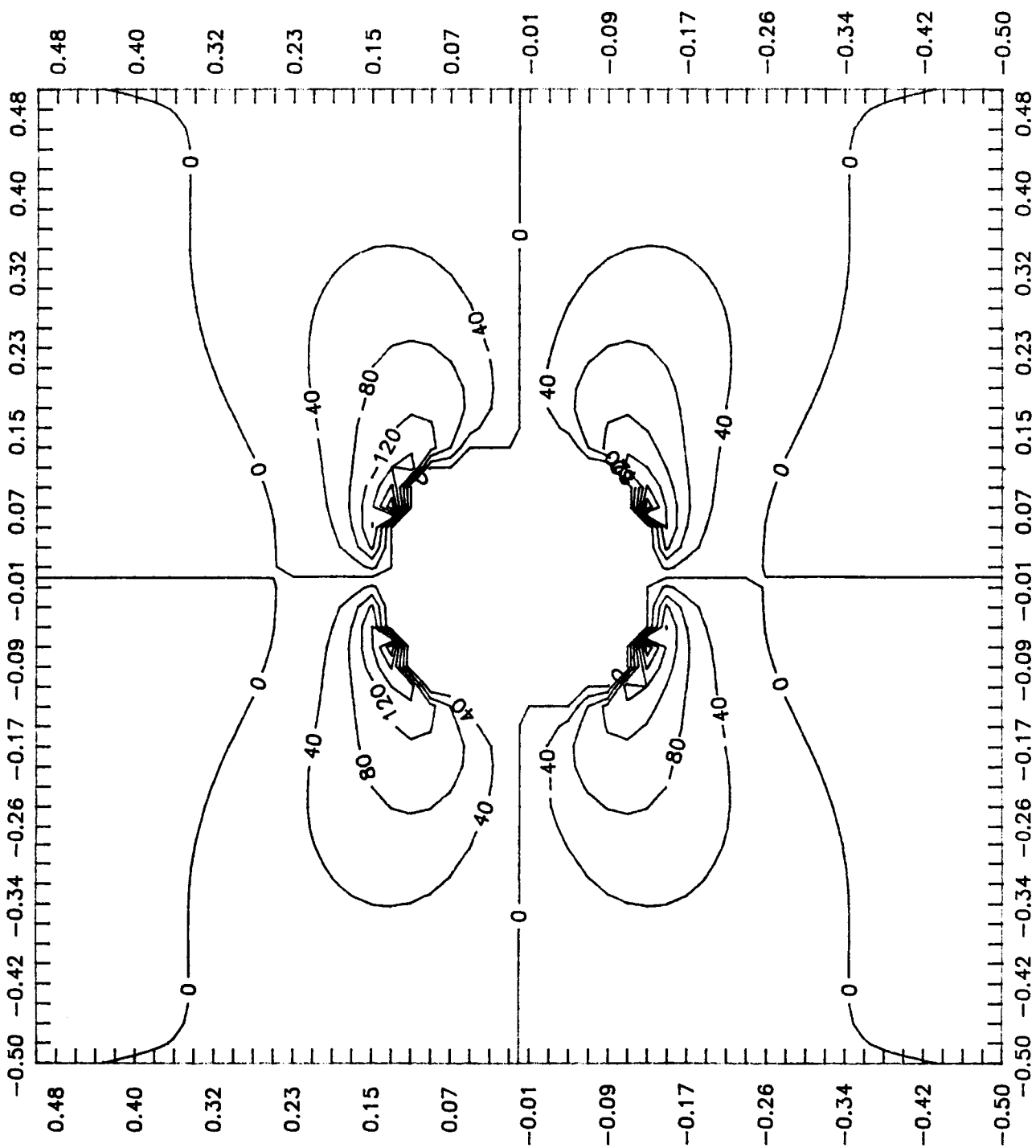
Figure 1, Circle — Stress in the x-direction

Figure 2, Circle — Stress in the y-direction
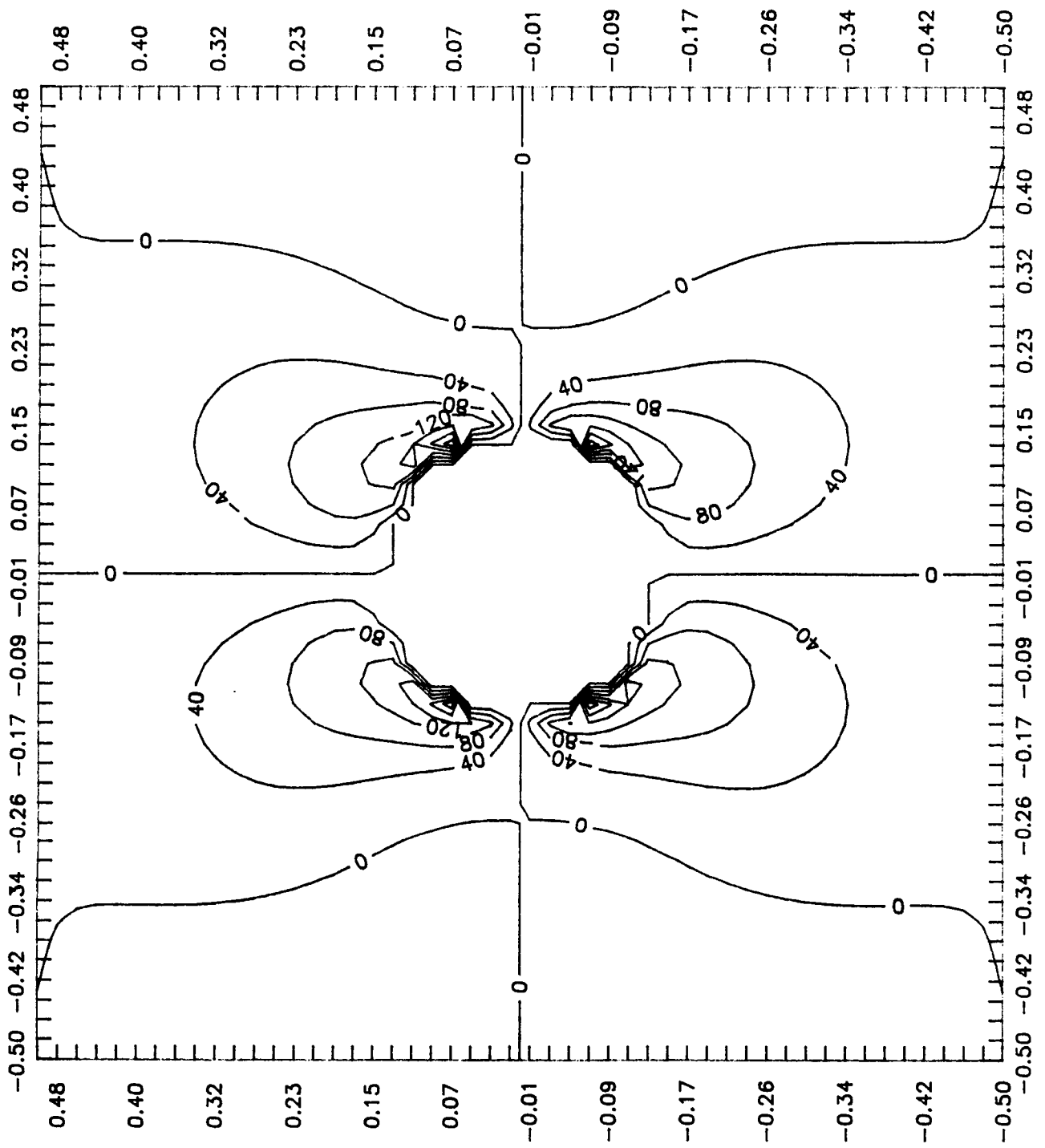
Figure 3, Shear Stress
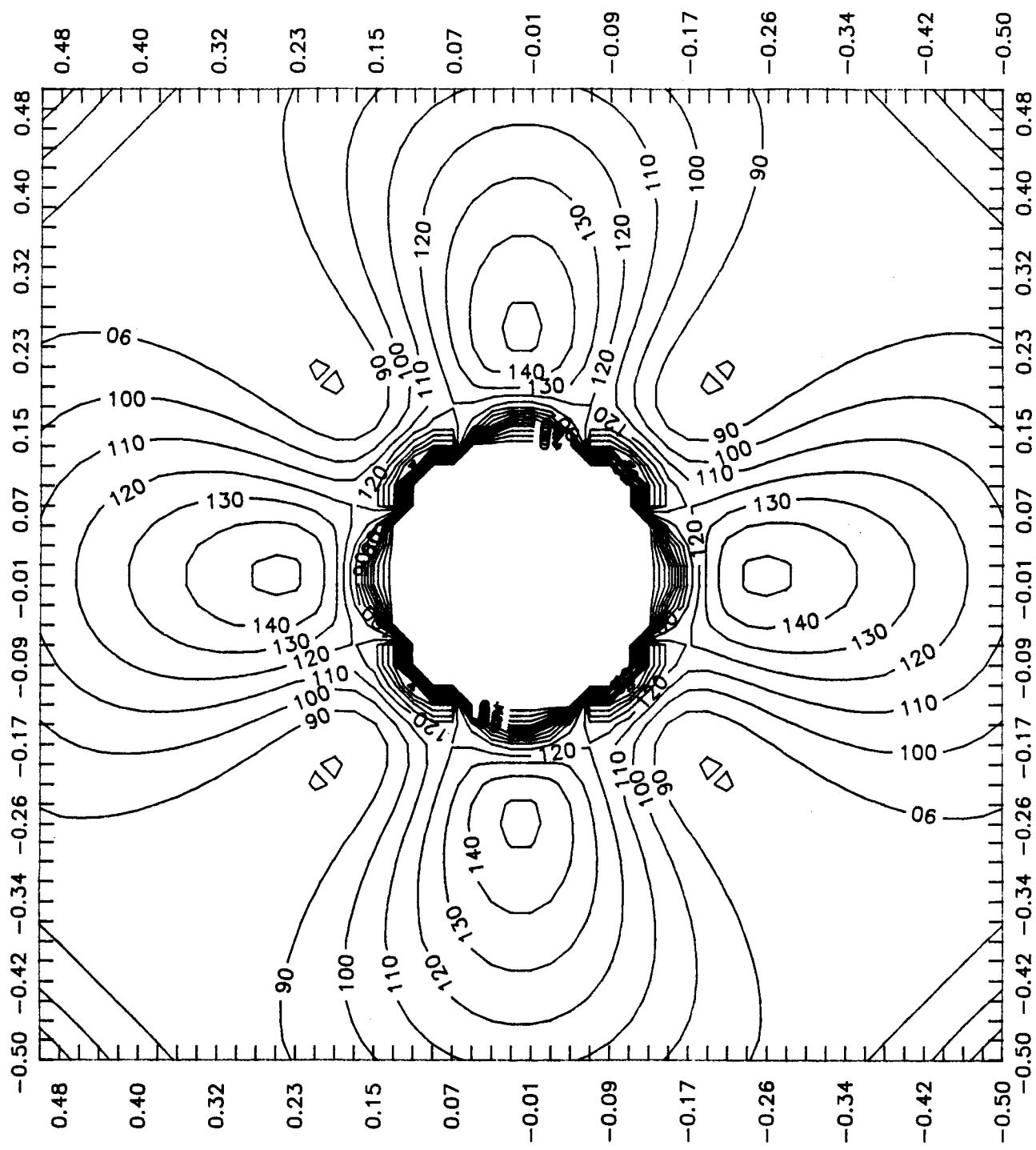
Figure 4, Circular Hole – Radius=0.25
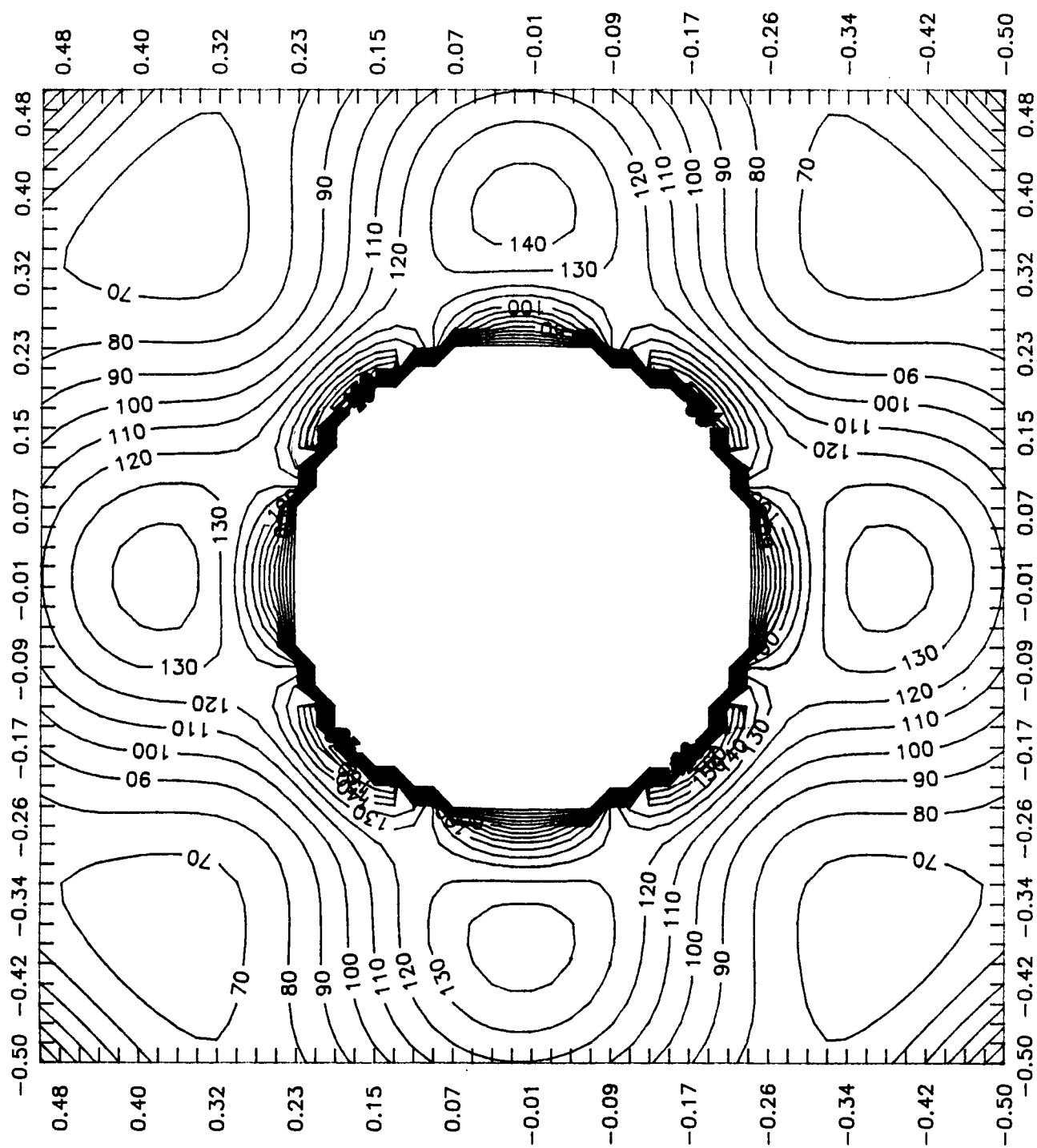
Figure 5, Circular Hole – 24 ply $\phi^\bullet$
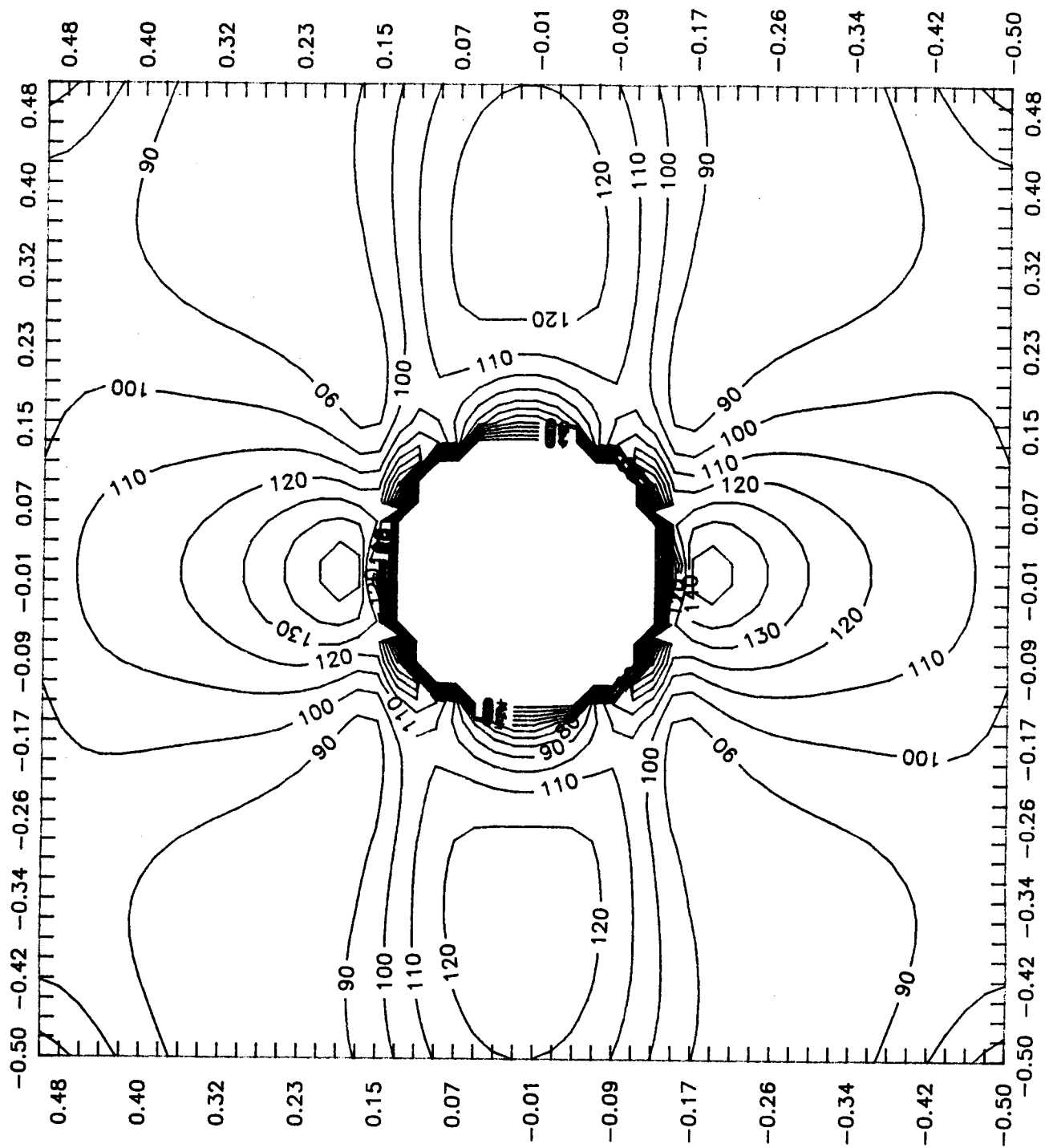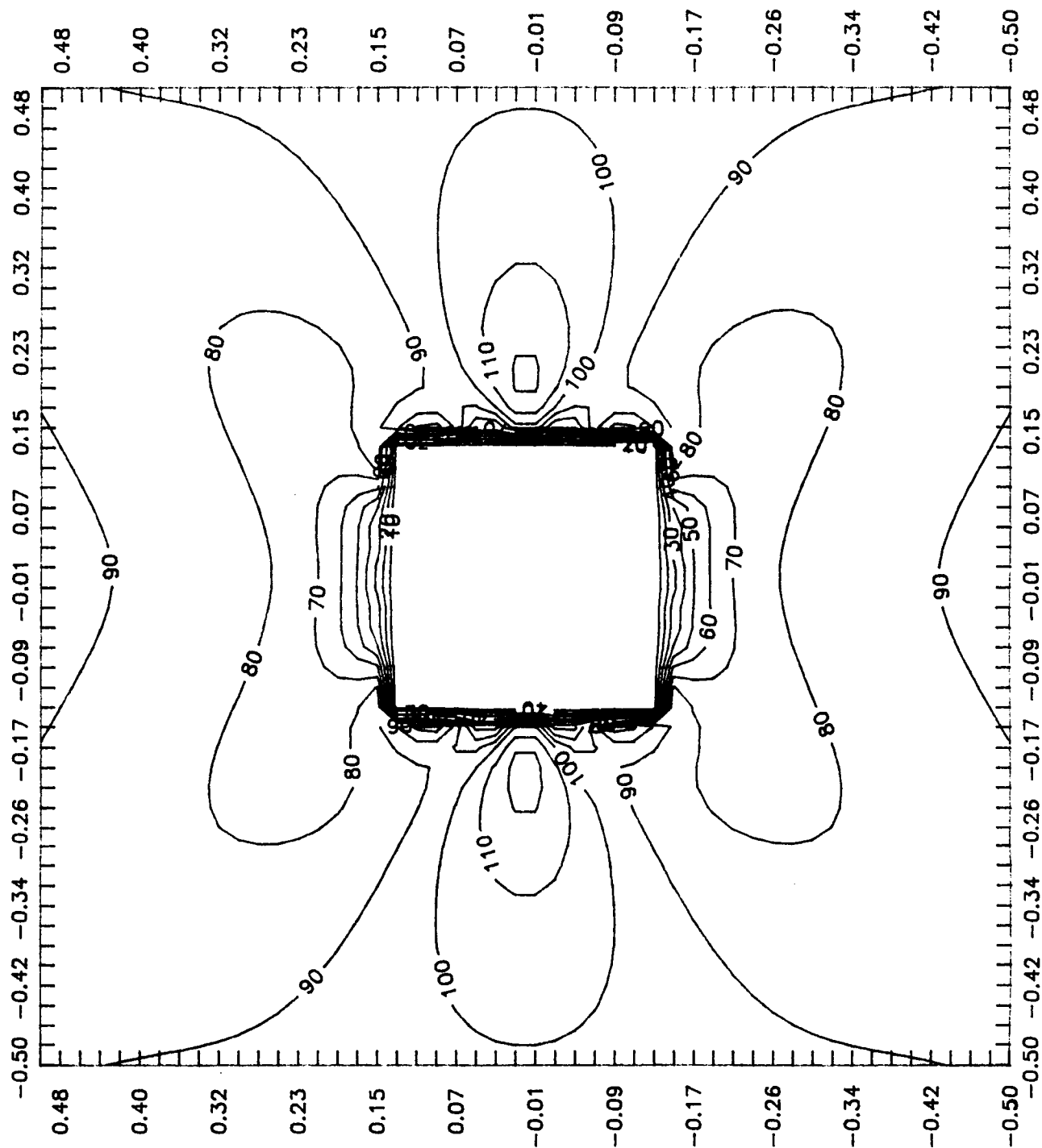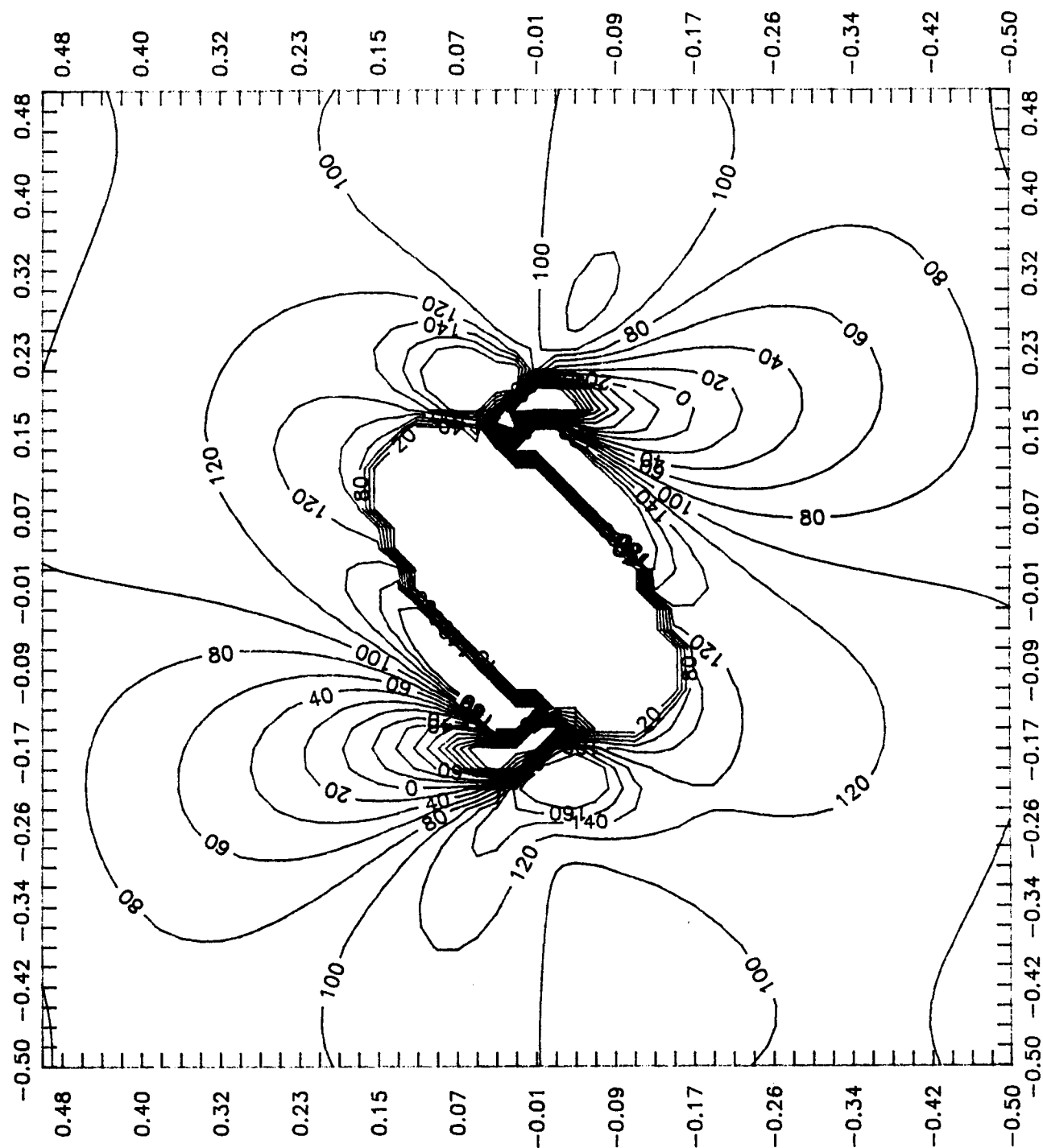
Figure 6, Elliptical Hole — R1=.2 R2=.1
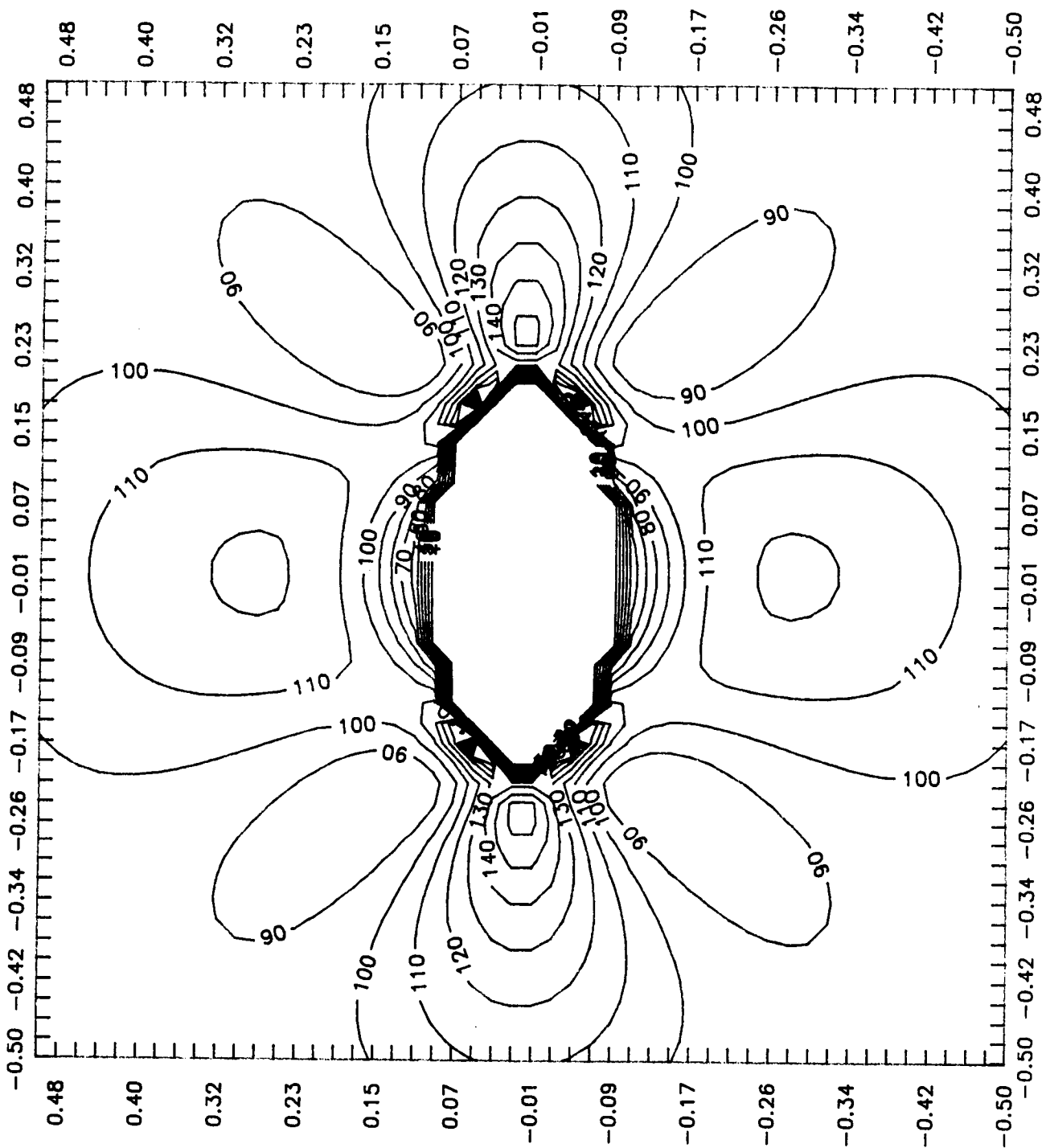
Figure 7, Square Hole L=W=.3

Figure 8, Ellipse (R1=.2,R2=.1) Rotated at 45°

Shear Stress along the x-axis
Hole Radius = .15

Shear Stress

Distance from hole to plate edge (y=0)

--■-- Complex Variables   --+-- Infinite Theory
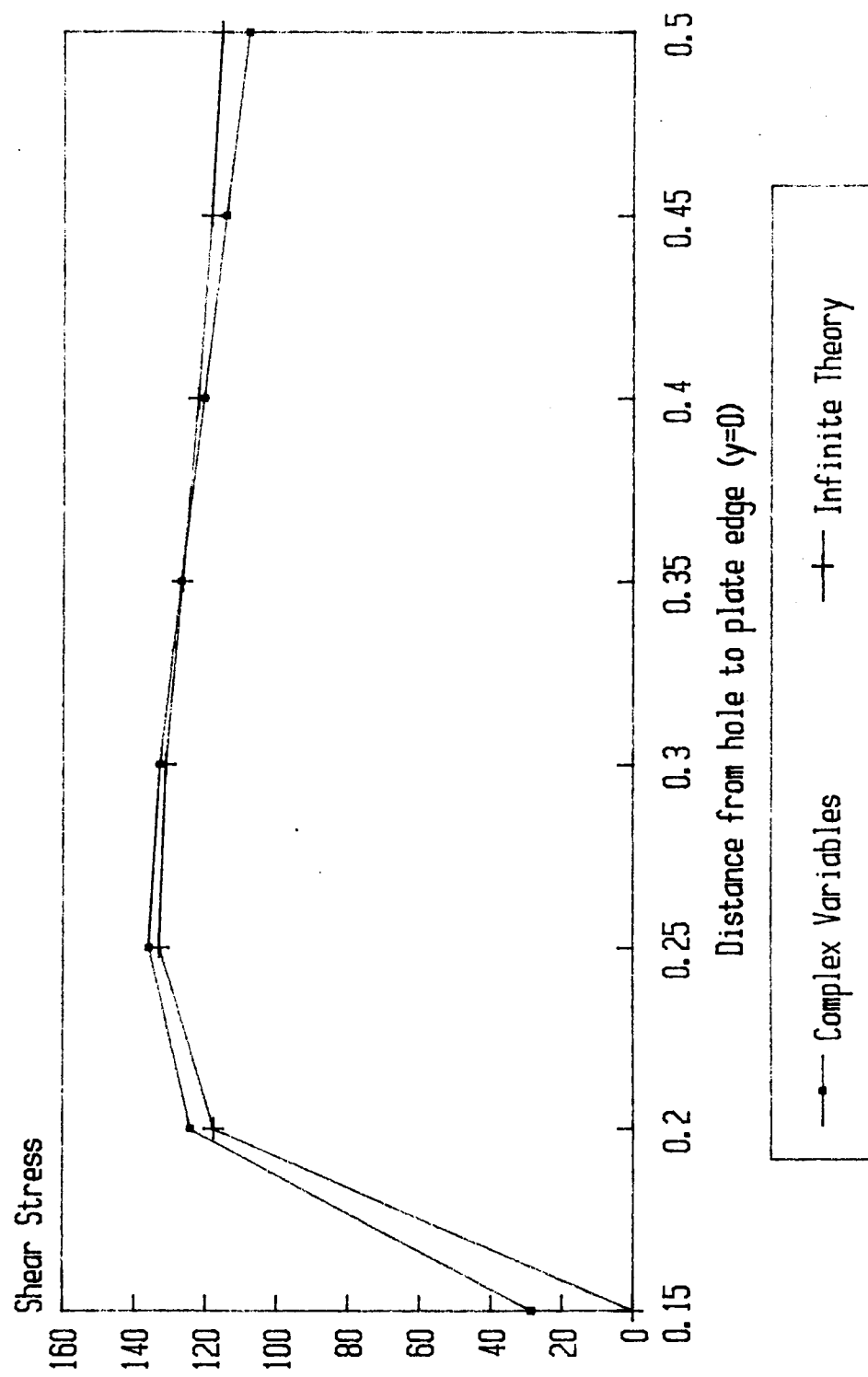
Figure 9

Shear Stress along the x-axis
Hole Radius = .10

Shear Stress

Distance from hole to plate edge (y=0)

— Complex Variables   — Infinite Theory
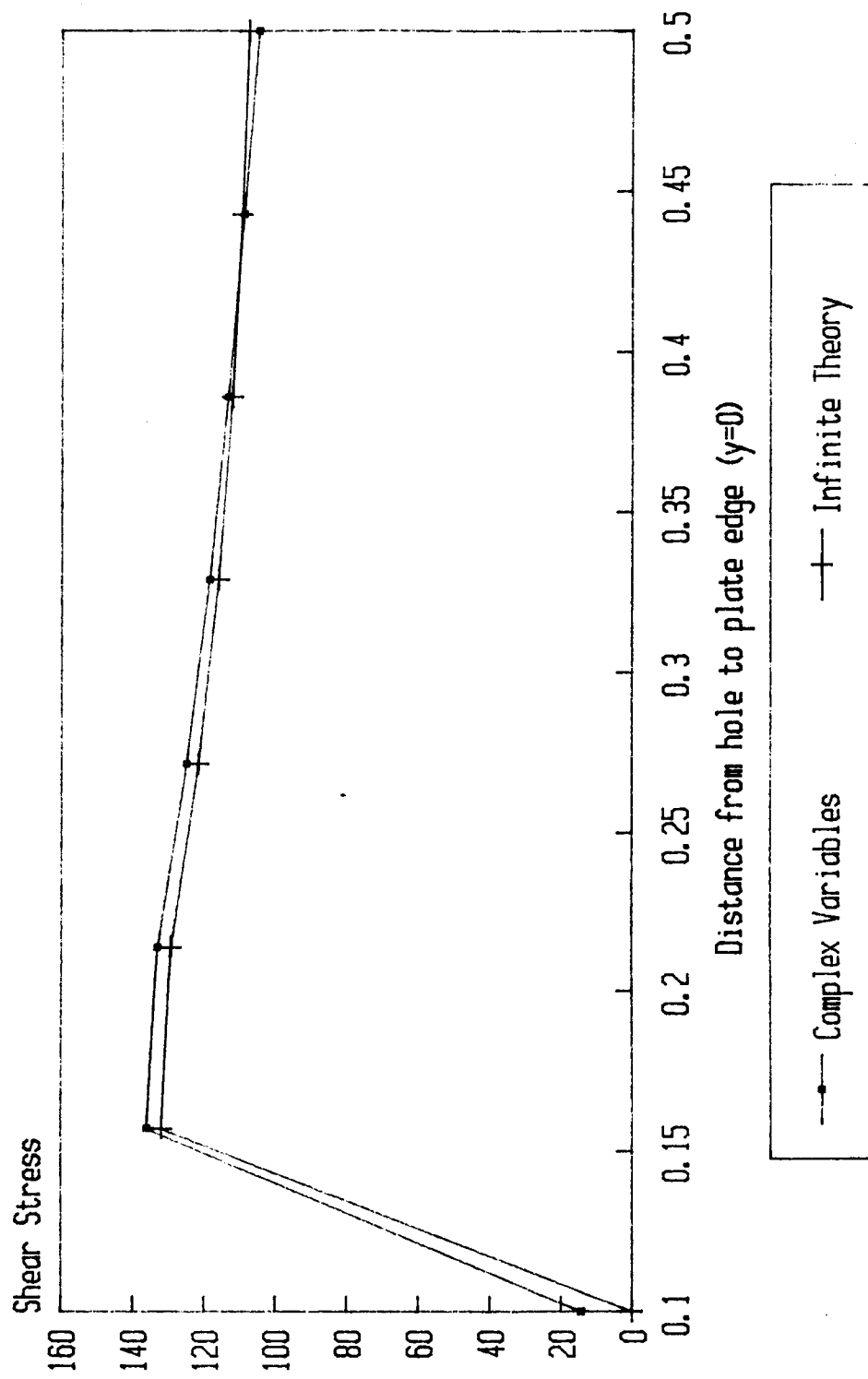
Figure 10

Shear Stress along the x-axis
Hole Radius = .05

Shear Stress

Distance from hole to plate edge (y=0)

—•— Complex Variables   —+— Infinite Theory
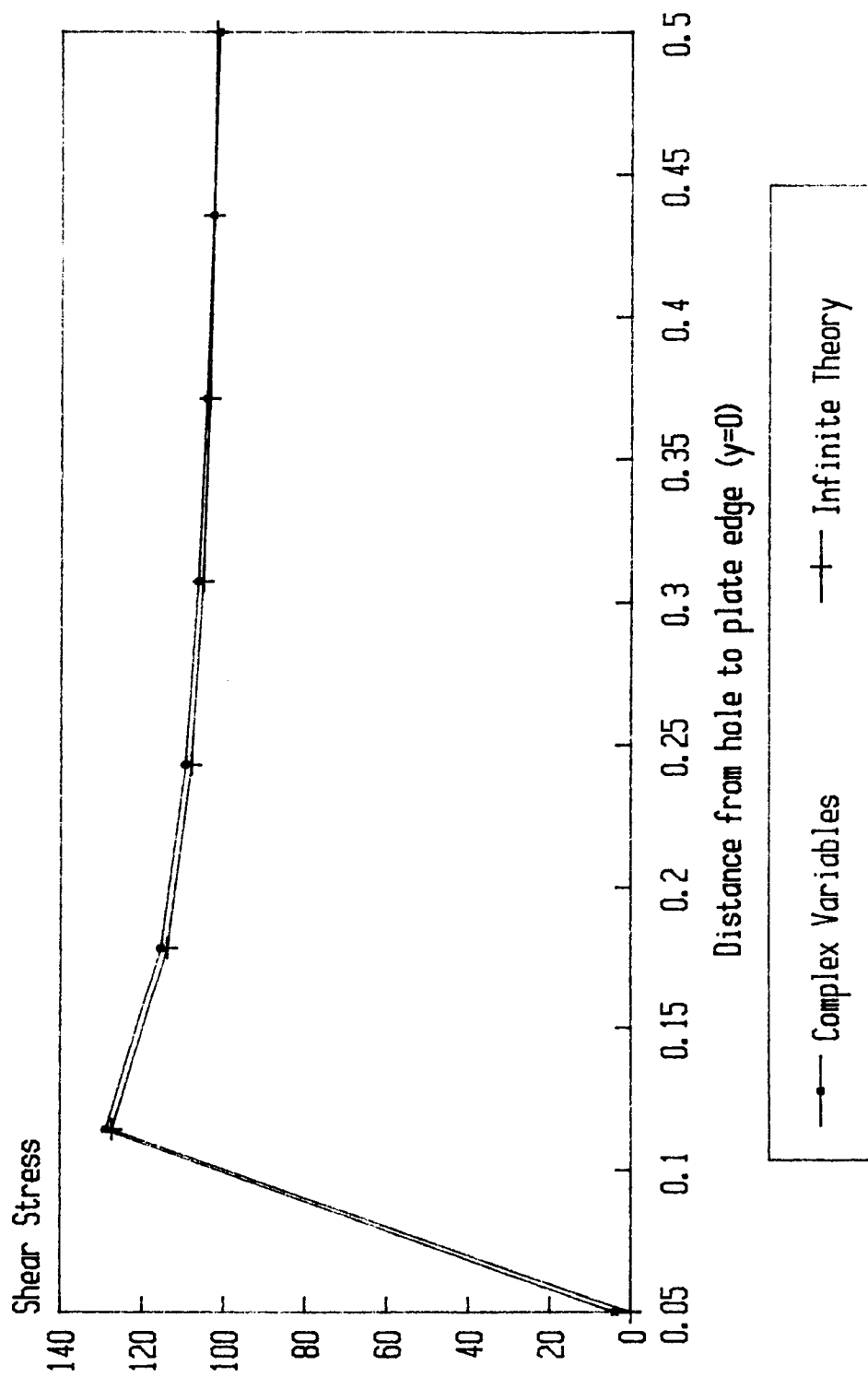
Figure 11

Shear Stress along the x-axis
Hole Radius = .01

Shear Stress

120

100

80

60

40

20

0

0.01   0.06   0.11   0.16   0.21   0.26   0.31   0.36   0.41   0.46

Distance from hole to plate edge (y=0)

—•— Complex Variables   —+— Infinite Theory
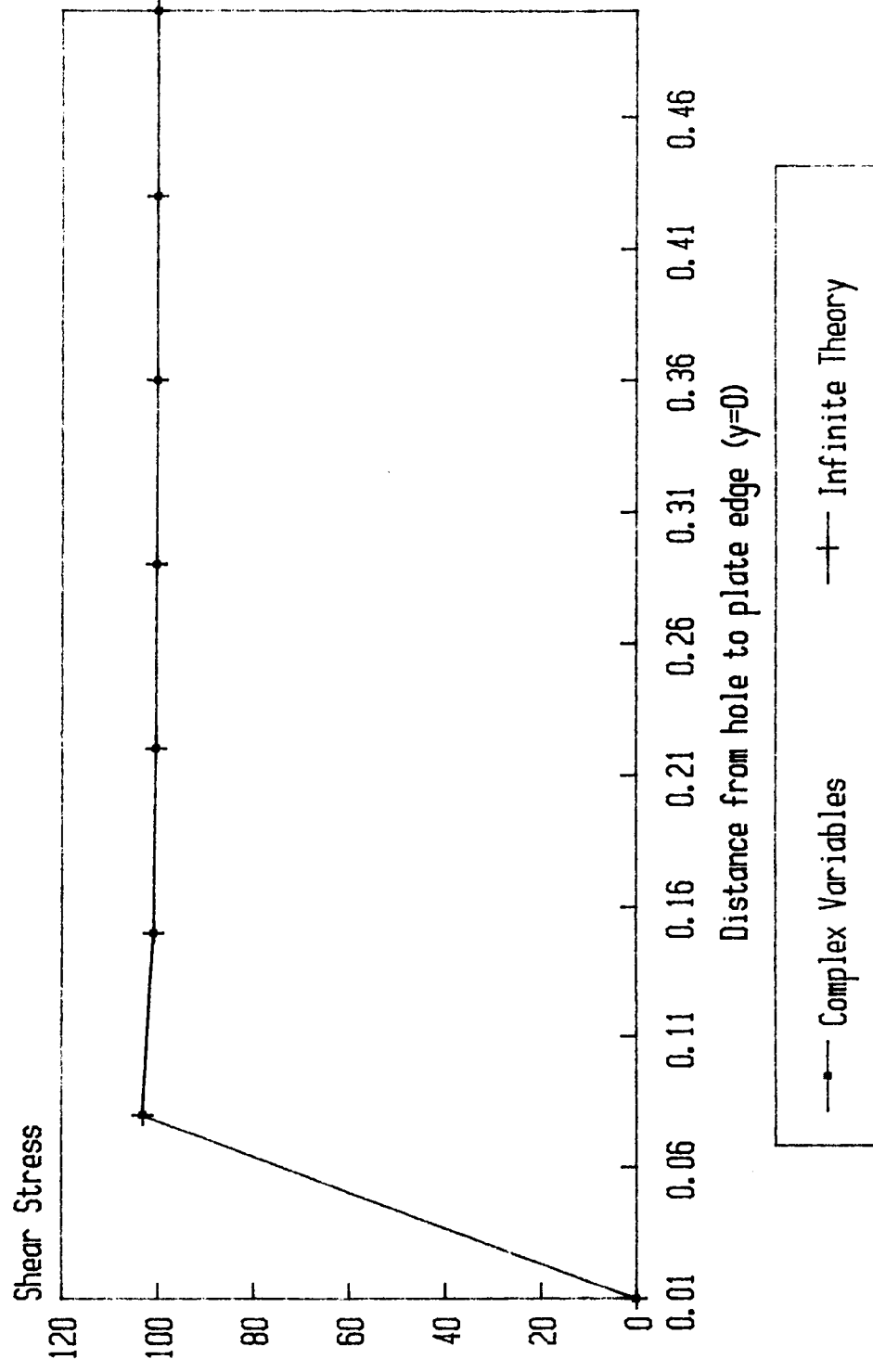
Figure 12

Stress in y-dir. vs. x (along y=0)
for 3 Hole Radius Sizes

Normal Stress in y-dir.

Distance from hole to plate edge (y=0)

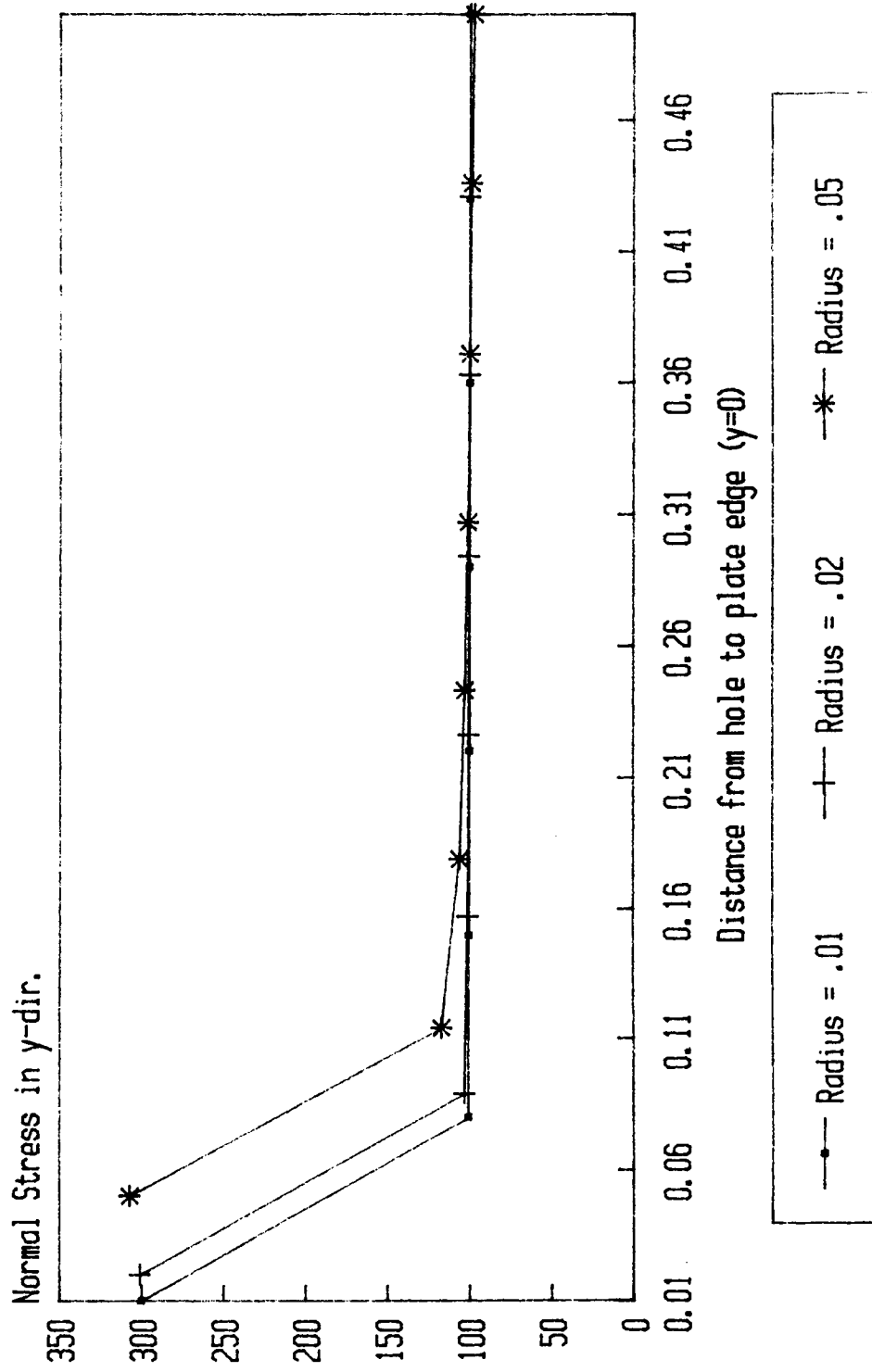— • — Radius = .01   — + — Radius = .02   — * — Radius = .05

Figure 13

Shear Stress along the x-axis
Varying the # of Series Terms

Figure 14